A Comparison of Ekman Pumping in Approximate Models of the Accelerating Planetary Boundary Layer

PETER R. BANNON

Department of Meteorology, The Pennsylvania State University, University Park, Pennsylvania

(Manuscript received 13 January 1997, in final form 27 August 1997)

ABSTRACT

Several theories of the planetary boundary layer that retain the flow accelerations in approximate form are compared. Two special test cases focus on the role of either local or convective accelerations. The semigeotriptic theory of Cullen predicts the boundary layer pumping most accurately for the cases and parameter range considered here.

1. Introduction

Ekman (1905) presented the classic geophysical model of the planetary boundary layer. This model consists of a force balance between the Coriolis, frictional, and pressure gradient forces in which a constant eddy diffusivity is employed. The model predicts a hodograph that veers with height with a cross-isobaric flow toward lower pressure near the surface that asymptotes to a geostrophic flow aloft. The ageostrophic component of the flow can be convergent and lead to rising motion at the top of the boundary layer. This so-called Ekman pumping is the primary mechanism whereby the interior flow feels the influence of the boundary layer (Charney and Eliassen 1949).

The Ekman model neglects the effect of the acceleration of the flow. Benton et al. (1964) presented solutions for a class of steady-state models that included the convective accelerations. Their findings show that Ekman theory overestimates the boundary layer pumping for cyclonic flow. Young (1973) found that Ekman theory also overestimates the pumping for cyclonic flow if the local acceleration terms are included.

A variety of theories have been advanced to approximate the equations of motion by eliminating gravity waves in order to describe a balanced motion. The purpose of this paper is to compare the effect of the various approximations on the boundary layer pumping. This comparison is accomplished for two test cases that are solved both with and without approximation. Comparison of these solutions helps us understand the role of various processes in the boundary layer response to flow acceleration.

Section 2 describes the theories. Section 3 presents the first of two cases. In this linear case the flow transience is retained by allowing the geostrophic wind to increase exponentially with time. This choice is a crude model of the growth of a front or a baroclinically unstable flow. Section 4 presents the results for the second test case for which the flow is assumed to be steady but the nonlinear convective accelerations are retained. Section 5 summarizes the findings.

2. The models

We consider the model atmosphere to be a semi-infinite Boussinesq fluid on an f plane with a Cartesian coordinate system. The effects of friction are incorporated using a constant eddy viscosity in the vertical. The flow is driven by a zonal pressure gradient force. The associated geostrophic wind in the meridional (y) direction is assumed to be

$$V_g = V_0\left(1 + \frac{x}{L}\right)e^{\sigma t}, \tag{2.1}$$

where V_0, L, and σ are constants. The subscript g denotes a geostrophic quantity. Here a positive value of σ models a growing geostrophic flow; a negative value models a decaying geostrophic flow. The atmosphere is horizontally unbounded. The linear dependence in the zonal (x) direction in (2.1) enables separable solutions. We assume V_0 is positive. Then a positive value of L models a cyclonic shear; a negative value models an anticyclonic shear.

We seek solutions for the velocity field, which is only a function of the zonal (x) and vertical (z) spatial co-

Corresponding author address: Dr. Peter R. Bannon, Department of Meteorology, The Pennsylvania State University, 503 Walker Building, University Park, PA 16802.
E-mail: bannon@ems.psu.edu

ordinates and of time (t). Then the horizontal momentum equations and the continuity equation become

$$\frac{Du}{Dt} - fv = -fV_g + \kappa\frac{\partial^2 u}{\partial z^2}, \tag{2.2}$$

$$\frac{Dv}{Dt} + fu = +\kappa\frac{\partial^2 v}{\partial z^2}, \tag{2.3}$$

$$\frac{\partial u}{\partial x} + \frac{\partial w}{\partial z} = 0, \tag{2.4}$$

where f is the constant Coriolis parameter (assumed positive), κ is the constant vertical eddy diffusivity, and the material derivative is

$$\frac{D}{Dt} \equiv \frac{\partial}{\partial t} + u\frac{\partial}{\partial x} + w\frac{\partial}{\partial z}. \tag{2.5}$$

Henceforth we refer to the set (2.2)–(2.4) as the nongeostrophic (NG) equations. The energetics are summarized by

$$\frac{D}{Dt}\left(\frac{u^2 + v^2}{2}\right) = uF_x + vF_y - fV_g u, \tag{2.6}$$

where

$$(F_x, F_y) = \kappa\frac{\partial^2(u, v)}{\partial z^2} \tag{2.7}$$

is the frictional force. Equation (2.6) states that changes in the kinetic energy of the wind arise from an imbalance between the work done by the frictional and by the pressure gradient forces.

Various approximations to these equations have been proposed in the geophysical literature. The Ekman equations simplify the horizontal momentum equations (2.2) and (2.3) by dropping the material derivatives to obtain

$$-fv = -fV_g + \kappa\frac{\partial^2 u}{\partial z^2}, \tag{2.8}$$

$$+fu = +\kappa\frac{\partial^2 v}{\partial z^2}. \tag{2.9}$$

We refer to the set (2.8), (2.9), and (2.4) as the Ekman equations, which are valid in quasigeostrophic (QG) theory (Pedlosky 1987) and whose solutions are well known. The energetics are

$$0 = uF_x + vF_y - fV_g u, \tag{2.10}$$

which implies that the loss of kinetic energy due to the frictional forces is compensated by the flow down the pressure gradient.

Wu and Blumen (1982) simplify the horizontal momentum equation of the NG set by making the geostrophic momentum (GM) approximation of Hoskins (1975). Specifically, they replace (2.2) and (2.3) with

$$-fv = -fV_g + \kappa\frac{\partial^2 u}{\partial z^2}, \tag{2.11}$$

$$\frac{DV_g}{Dt} + fu = +\kappa\frac{\partial^2 v}{\partial z^2}, \tag{2.12}$$

which retains only the terms associated with the acceleration of the geostrophic wind V_g. The energy equation takes the form

$$\frac{D}{Dt}\left(\frac{V_g^2}{2}\right) = V_g F_y - fV_g u. \tag{2.13}$$

Here the kinetic energy is approximated by that of the geostrophic wind and the work done by the frictional forces is only that associated with the geostrophic flow.

Cullen (1989) suggests the use of

$$\frac{Dv}{Dt} + fu = +\kappa\frac{\partial^2 v}{\partial z^2}, \tag{2.14}$$

in place of (2.12). We refer to this set [(2.4), (2.11), and (2.14)] as the semigeotriptic (SG) approximation. [Johnson (1966) introduced the term geotriptic to refer to the Ekman balance between frictional, pressure gradient, and Coriolis forces.] Cullen shows that this semigeotriptic set has a statement of energy conservation of the form

$$\frac{D}{Dt}\left(\frac{v^2}{2}\right) = uF_x + vF_y - fV_g u, \tag{2.15}$$

and the kinetic energy is approximated by only that of the meridional wind.

More recently Tan and Wu (1993) suggest an Ekman momentum (EM) approximation that uses

$$\frac{Du_E}{Dt} - fv = -fV_g + \kappa\frac{\partial^2 u}{\partial z^2}, \tag{2.16}$$

$$\frac{DV_E}{Dt} + fu = +\kappa\frac{\partial^2 v}{\partial z^2}, \tag{2.17}$$

in place of (2.2) and (2.3). Here (U_E, V_E) is the solution to the Ekman equations (2.8) and (2.9). The energetics of this set are given by

$$\frac{D}{Dt}\left(\frac{U_E^2 + V_E^2}{2}\right) = U_E F_x + V_E F_y - fV_g U_E + fvU_E - fuV_E. \tag{2.18}$$

This equation is similar to (2.6) except that the kinetic energy and frictional working are evaluated using the Ekman wind. However, the last two terms in (2.18) are unphysical Coriolis contributions; they represent additional energy sources/sinks with no counterpart in the nongeostrophic energy equation (2.6).

3. Linear transient case

The first test case of the approximate equations considers the geostrophic flow (2.1) in the small amplitude

limit for which the material derivative (2.5) may be replaced with the local derivative

$$\frac{D}{Dt} \to \frac{\partial}{\partial t}. \tag{3.1}$$

Then the governing equations are linear and analytic solutions are readily found.

We first solve the nongeostrophic problem and then compare this complete solution with that obtained using the various approximate equations. Setting $\kappa = 0$ in (2.2) and (2.3) with (3.1) yields the inviscid (denoted with the subscript I) equations, which have the solution

$$u_I = -\frac{\tau}{1 + \tau^2} V_g \tag{3.2a}$$

$$v_I = +\frac{1}{1 + \tau^2} V_g \tag{3.2b}$$

$$w_I = \frac{\tau(z/L)e^{\sigma t}}{1 + \tau^2} V_0, \tag{3.2c}$$

where

$$\tau \equiv \sigma/f \tag{3.3}$$

is a nondimensional measure of the ageostrophy introduced by the time dependence of the geostrophic wind (2.1). In writing (3.2) we have neglected any transient solution (e.g., an inertial oscillation) associated with unbalanced initial conditions. We do not consider here the general initial value problem but assume the time dependence (2.1).

The complete solution with friction may be written in the form

$$u = u_I + V_g \hat{u}(\eta) \tag{3.4a}$$

$$v = v_I + V_g \hat{v}(\eta) \tag{3.4b}$$

$$w = w_I + \frac{V_0 e^{\sigma t}}{L}\left(\frac{2\kappa}{f}\right)^{1/2} \hat{w}(\eta), \tag{3.4c}$$

where

$$z = \left(\frac{2\kappa}{f}\right)^{1/2} \eta \tag{3.5}$$

defines the nondimensional vertical coordinate η in the boundary layer. The velocity fields with a circumflex in (3.4) are nondimensional.

It is straightforward to show that substitution of (3.4) into (2.2) and (2.3) with (3.1) yields a single equation for the nondimensional zonal velocity field:

$$\frac{d^4\hat{u}}{d\eta^4} - 4\tau\frac{d^2\hat{u}}{d\eta^2} + 4(1 + \tau^2)\hat{u} = 0. \tag{3.6}$$

The solution to (3.6) that is bounded at $\eta = \infty$ has the form

$$\hat{u} = A_+ e^{\lambda_+ \eta} + A_- e^{\lambda_- \eta}, \tag{3.7}$$

where

$$\lambda_\pm = -\sqrt{r}\, e^{\pm i\theta/2} \tag{3.8}$$

are the two roots of the equation

$$\lambda^2 = 2(\tau \pm i) \tag{3.9}$$

with negative real parts. Here

$$r = 2\sqrt{1 + \tau^2}, \tag{3.10a}$$

$$\theta = \tan^{-1}\left(\frac{1}{\tau}\right) \quad \text{for } \tau > 0,$$

$$\theta = \pi - \tan^{-1}\left|\frac{1}{\tau}\right| \quad \text{for } \tau < 0. \tag{3.10b}$$

The constants A_+ and A_- in (3.7) are determined from the no-slip boundary conditions at $\eta = 0$. The result is

$$A_\pm = \frac{\tau \pm (-i)}{2(1 + \tau^2)}. \tag{3.11}$$

The solution for the wind field may be written as

$$\frac{u}{V_g} = -\frac{1}{1 + \tau^2} e^{-\gamma\eta} \sin\alpha\eta - \frac{\tau}{1 + \tau^2} \times (1 - e^{-\gamma\eta} \cos\alpha\eta) \tag{3.12a}$$

$$\frac{v}{V_g} = +\frac{1}{1 + \tau^2}(1 - e^{-\gamma\eta} \cos\alpha\eta) - \frac{\tau}{1 + \tau^2} \times e^{-\gamma\eta} \sin\alpha\eta, \tag{3.12b}$$

where

$$\gamma = \sqrt{r} \cos\left(\frac{\theta}{2}\right), \qquad \alpha = \sqrt{r} \sin\left(\frac{\theta}{2}\right). \tag{3.13}$$

Inspection of (3.12) indicates that the total solution is the sum of two spirals. The first terms in (3.12) represent a spiral for the meridional interior flow (3.2b), the second terms for the zonal interior flow (3.2a). For each spiral $r^{1/2}$ is the decay rate of the boundary layer flow while $\theta/2$ is the crossing angle (or angle that the surface flow makes to the left of the interior flow). From (3.10a) the decay rate increases for both accelerating or decelerating flow, implying a shallower boundary layer. From (3.10b) the crossing angle for the individual spiral is greater for decelerating flow ($\tau < 0$) than accelerating flow ($\tau > 0$). However, the crossing angle relative to the isobars for the total solution is typically larger for the accelerating case whose isallobaric component is down the pressure gradient.

The nondimensional vertical motion field at the top of the boundary layer is found by vertically integrating the continuity equation (2.4) to be

$$\hat{w}(\eta = \infty) \equiv W_{\text{NG}} = \frac{\sin(\theta/2)}{\sqrt{2}(1 + \tau^2)^{5/4}} - \frac{\tau \cos(\theta/2)}{\sqrt{2}(1 + \tau^2)^{5/4}}. \tag{3.14}$$

The two terms in (3.14) correspond to the two spirals: the first for the interior meridional flow, the second for the interior zonal flow. Note that the interior flow (3.2) contributes the factor $(1 + \tau^2)^{-1}$ while the reduction in the decay rate of the spiral contributes a factor $(1 + \tau^2)^{-1/4}$.

The preceding analysis has been for the nongeostrophic equations. We interpret these findings through comparison with the parallel analyses for the various approximate equations. The quasigeostrophic solution may be found from the nongeostrophic one by taking the limit as τ tends to 0. Then the inviscid QG solutions [cf. (3.2)] consist of only the geostrophic flow $v = V_g$. The QG approximation overestimates the meridional wind and fails to include the isallobaric zonal component (3.2a). The QG vertical motion field has no inviscid isallobaric component like (3.2c), and the pumping term (3.14) reduces to the well-known value, given in the present notation as

$$W_{\mathrm{QG}} = \frac{1}{2}, \tag{3.15}$$

which is independent of the ageostrophic parameter τ.

The solutions of the geostrophic momentum equations differ from the inviscid NG solution in that the $O(\tau^2)$ terms in (3.2) are dropped. In contrast with the QG approximation, the GM solution retains an isallobaric flow that is subject to the no-slip boundary condition. This feature is its major improvement over the QG result. The vertical motion field is the sum of (3.2c) [with the $O(\tau^2)$ term neglected], and the approximation to (3.14) is

$$W_{\mathrm{GM}} = \frac{1}{2} - \frac{1}{2}\tau. \tag{3.16}$$

The transience decreases the boundary layer pumping in a growing ($\sigma > 0$) disturbance but increases the pumping in a decaying ($\sigma < 0$) disturbance. This behavior shows that friction reduces the isallobaric component of the flow in the boundary layer, thereby reducing the isallobaric convergence into a deepening low pressure system (Young 1973).

The solution for the EM approximation is identical to the result of Young (1973) that

$$W_{\mathrm{EM}} = \frac{1}{2} - \frac{3}{4}\tau, \tag{3.17}$$

which was derived using a series expansion in the Rossby number τ. The result (3.17) uses (2.16) and (2.17). If, following Tan and Wu (1993), we make the additional assumption that the frictional terms may be evaluated using the Ekman velocity field, then the boundary layer pumping is identical to the GM result (3.16).

The SG pumping is given by

$$W_{\mathrm{SG}} = \frac{(1 - \tau^2/2)\sin(\beta/2)}{\sqrt{2}\,(1 - \tau^2/4)^{1/2}} - \frac{\tau\cos(\beta/2)}{\sqrt{2}}, \tag{3.18}$$

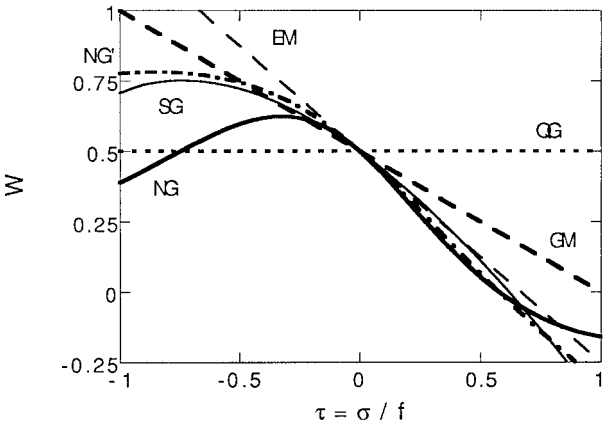

FIG. 1. Nondimensional boundary layer pumping, W, as a function of the ageostrophic parameter $\tau = \sigma/f$ for the quasigeostrophic (QG), semigeotriptic (SG), geostrophic momentum (GM), and Ekman momentum (EM) approximations, the exact nongeostrophic (NG), and the approximate nongeostrophic result (NG′) result. Here σ is the growth rate of the geostrophic wind.

where

$$\beta = \tan^{-1}\left(\frac{\sqrt{4 - \tau^2}}{\tau}\right) \quad \text{for } \tau > 0,$$
$$\beta = \pi - \tan^{-1}\left|\frac{\sqrt{4 - \tau^2}}{\tau}\right| \quad \text{for } \tau < 0. \tag{3.19}$$

Thus the SG theory contains a better estimate of the effect of nongeostrophy on the vertical structure of the boundary layer.

Figure 1 compares the boundary layer pumping terms for the various approximations. All the solutions yield the Ekman result $W = 1/2$ for the steady-state case $\sigma = 0$. The slopes of the curves at $\tau = 0$ are -0.750 for the nongeostrophic and Ekman momentum solutions, -0.625 for the semigeotriptic solution, and -0.500 for the geostrophic momentum solution. In general, the approximations tend to overestimate the boundary layer pumping. A major reason for this overestimation is that the approximate solutions overestimate the interior flow. Mathematically they neglect the factor $(1 + \tau^2)^{-1}$ in (3.2). The NG solution (3.14) without this factor is plotted as the dashed-dotted curve labeled NG′ in Fig. 1. Only the SG approximation contains an estimate of the effect of the transience on the boundary layer decay rate and crossing angle. For a growing pressure gradient, $\tau > 0$, the EM and SG approximations are the better of the group compared. For a decaying pressure gradient, the SG approximation is better than most, but the error increases for large negative τ.

4. Nonlinear steady-state case

The second test case of the approximate equations considers the geostrophic flow (2.1) to have finite amplitude but to be invariant with time. Then $\sigma = 0$ and

the material derivative may be replaced with the convective derivative

$$\frac{D}{Dt} \rightarrow u\frac{\partial}{\partial x} + w\frac{\partial}{\partial z}. \tag{4.1}$$

We again first solve the nongeostrophic problem and then compare this complete solution with that obtained using the various approximations. To solve (2.2) and (2.3) with (4.1), we first partition the flow variables into geostrophic and ageostrophic components

$$u = V_0(1 + x/L)u_a(z) \tag{4.2a}$$

$$v = V_0(1 + x/L)[1 + v_a(z)] \tag{4.2b}$$

$$w = \frac{V_0}{L}\left(\frac{2\kappa}{f}\right)^{1/2} w_a(z). \tag{4.2c}$$

Here the fields are separable in their x and z dependence and the nondimensional vertical structure functions of the ageostrophic flow components are denoted with a subscript, a. Solving for the ageostrophic zonal wind yields

$$\frac{\partial^4 u_a}{\partial \eta^4} - 4\mathrm{Ro}w_a\frac{\partial^3 u_a}{\partial \eta^3} + (-2\mathrm{Ro}u_a + 4\mathrm{Ro}^2 w_a^2)\frac{\partial^2 u_a}{\partial \eta^2} + \left(-2\mathrm{Ro}\frac{\partial u_a}{\partial \eta} + 8\mathrm{Ro}^2 u_a w_a\right)\frac{\partial u_a}{\partial \eta} + 4(1 + \mathrm{Ro} + \mathrm{Ro}^2 u_a^2)u_a = 0, \tag{4.3}$$

where the Rossby number, $\mathrm{Ro} = V_0/fL$, is a nondimensional measure of the ageostrophy of the flow. Note that section 3 considers the limit of vanishing Rossby number. Since w_a is related to u_a by

$$w_a(\eta) = -\int_o^\eta u_a(\eta')\, d\eta', \tag{4.4}$$

(4.3) is a single equation for the vertical structure function of the ageostrophic zonal wind u_a.

The differential equation (4.3) is highly nonlinear and its solution is obtained numerically. We use the method of Lindzen and Kuo (1969) to solve (4.3) and similar equations. The equation is solved iteratively with the coefficients taken to be known functions given by the earlier iteration. The first guess is found by solving the quasigeostrophic problem

$$\frac{\partial^4 u_a}{\partial \eta^4} + 4u_a = 0. \tag{4.5}$$

Note that (4.3) reduces to (4.5) in the limit as Ro tends to zero.

The semigeotriptic version of (4.3) is

$$\frac{\partial^4 u_a}{\partial \eta^4} - 2\mathrm{Ro}w_a\frac{\partial^3 u_a}{\partial \eta^3} + (-2\mathrm{Ro}u_a)\frac{\partial^2 u_a}{\partial \eta^2} + 4(1 + \mathrm{Ro})u_a = 0, \tag{4.6}$$

the geostrophic momentum version is

$$\frac{\partial^4 u_a}{\partial \eta^4} + 4(1 + \mathrm{Ro})u_a = 0, \tag{4.7}$$

and the Ekman momentum version is

$$\frac{\partial^4 u_a}{\partial \eta^4} - 4\mathrm{Ro}w_a\frac{\partial^3 u_E}{\partial \eta^3} + (-2\mathrm{Ro}u_E)\frac{\partial^2 u_a}{\partial \eta^2} - 2\mathrm{Ro}\frac{\partial u_E}{\partial \eta}\frac{\partial u_a}{\partial \eta} + 4(1 + \mathrm{Ro})u_a = 0. \tag{4.8}$$

Comparison of (4.7) with (4.3) indicates that the geostrophic momentum approximation can be derived from the nongeostrophic equation if the nonlinear terms are neglected. In contrast, reduction of (4.3) to the semigeotriptic result (4.6) is not readily apparent by, say, the neglect of $O(\mathrm{Ro}^2)$ terms. The EM result (4.8) is found from the NG equation by dropping the $O(\mathrm{Ro}^2)$ terms and evaluating some of the functions with their Ekman values.

Figure 2 compares the boundary layer pumping predictions for the various approximations. The NG results are consistent with the analytic series solution of Benton et al. (1964). This agreement provides verification of the numerical method. All the solutions yield the Ekman result of 1/2 for the case of no shear ($L = \infty$). Qualitatively each theory predicts an increase in the pumping for anticyclonic ($\mathrm{Ro} < 0$) and a decrease for cyclonic shear ($\mathrm{Ro} > 0$). [Note that the sign of the pumping, denoting either ascent or descent, is given by the coefficient in (4.2c).] The SG and EM theories track the behavior of the exact NG result slightly better than does the GM theory. The approximations are better for cyclonic than for anticyclonic shear.

The QG pumping is a constant, $W_{\mathrm{QG}} = 1/2$, and shows no effects of the flow acceleration. The GM approximation only allows for the zonal advection of the geostrophic meridional wind. Wu and Blumen (1982) show that this meridional acceleration decreases (increases) the cross-isobaric flow and the depth of the boundary layer for cyclonic (anticyclonic) flow. The analytic solution of (4.7) implies a pumping of the form

$$W_{\mathrm{GM}} = \frac{1}{2(1 + \mathrm{Ro})^{3/4}}. \tag{4.9}$$

Figure 2 shows that this approximation overestimates the effect of the acceleration on the pumping. In con-

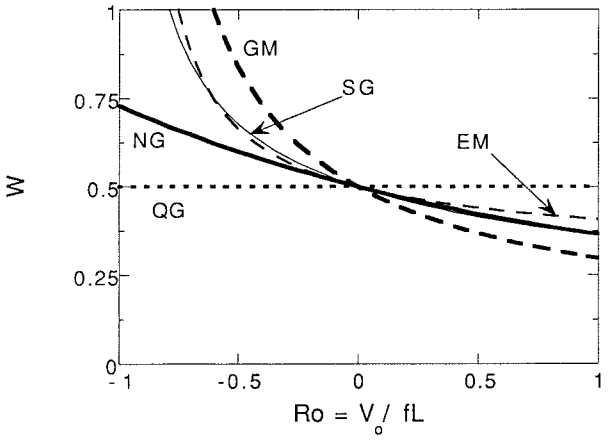

FIG. 2. Nondimensional boundary layer pumping, W, as a function of the ageostrophic parameter $\mathrm{Ro} = V_0/fL$ for the quasigeostrophic (QG), semigeotriptic (SG), geostrophic momentum (GM), and Ekman momentum (EM) approximations, and the exact nongeostrophic (NG) result. Here $V_0 > 0$ is the amplitude of the geostrophic wind and L is its horizontal scale (positive for cyclonic and negative for anticyclonic linear shear).

trast, the GM case includes the full meridional acceleration (i.e., both the zonal and vertical advection of the meridional wind) and produces closer agreement with the NG case. The difference between the SG and NG cases arise from the neglect of the zonal acceleration by the former. This neglect is significant only for anticyclonic flow. The EM approximation, which includes the acceleration of the Ekman wind, predicts a pumping comparable to the SG approximation.

5. Conclusions

We have tested three different approximate sets of planetary boundary equations that include the flow acceleration. Two test cases isolate the effect of the approximations in terms of the local and convective accelerations. Despite the special nature of these test cases, the results are believed to be representative. All the theories capture qualitatively the reduction of the boundary layer pumping for a growing geostrophic flow and for a cyclonic geostrophic flow.

All the results presented here have used the no-slip lower boundary condition. Use of the Taylor (1915) condition that the surface stress is parallel to the wind leads to similar qualitative behavior of the approximate theories as presented here. Quantitatively the boundary layer pumping is reduced with the Taylor condition.

The semigeotriptic theory of Cullen (1989) is the most accurate of the approximations over the range of ageostrophy tested (see Figs. 1 and 2). The Ekman momentum theory of Tan and Wu (1993) has similar accuracy except for the decelerating flow case (see Fig. 1 for $\tau < 0$) but its energy equation contains spurious Coriolis contributions. It should be noted that both the two- and three-dimensional versions of Cullen's theory produce the same results for the two-dimensional test cases investigated here. Further work should consider three-dimensional tests.

Acknowledgments. Partial financial support was provided by the National Science Foundation (NSF) under NSF Grant ATM-9424462.

REFERENCES

Benton, G. S., F. B. Lipps, and S.-Y. Tuann, 1964: The structure of the Ekman layer for geostrophic flows with lateral shear. *Tellus,* **16,** 186–199.

Charney, J. G., and A. Eliassen, 1949: A numerical method for predicting the perturbation of the middle-latitude westerlies. *Tellus,* **1,** 38–54.

Cullen, M. J. P., 1989: On the incorporation of atmospheric boundary layer effects into a balanced model. *Quart. J. Roy. Meteor. Soc.,* **115,** 1109–1131.

Ekman, V. W., 1905: On the influence of the earth's rotation on ocean currents. *Arch. Math. Astron. Phys.,* **2** (11), 1–53.

Hoskins, B. J., 1975: The geostrophic momentum approximation and the semi-geostrophic equations. *J. Atmos. Sci.,* **32,** 233–242.

Johnson, W. B., 1966: The geotriptic wind. *Bull. Amer. Meteor. Soc.,* **47,** 982.

Lindzen, R. S., and H. L. Kuo, 1969: A reliable method for the numerical integration of a large class of ordinary and partial differential equations. *Mon. Wea. Rev.,* **97,** 732–734.

Pedlosky, J., 1987: *Geophysical Fluid Dynamics.* Springer-Verlag, 710 pp.

Tan, Z., and R. Wu, 1993: The Ekman momentum approximation and its application. *Bound.-Layer Meteor.,* **68,** 193–199.

Taylor, G. I., 1915: Eddy motion in the atmosphere. *Philos. Trans. Roy. Soc. London,* **A215,** 1–26.

Wu, R., and W. Blumen, 1982: An analysis of Ekman boundary layer dynamics incorporating the geostrophic momentum approximation. *J. Atmos. Sci.,* **39,** 1774–1782.

Young, J. A., 1973: A theory for isallobaric air flow in the planetary boundary layer. *J. Atmos. Sci.,* **30,** 1584–1592.